

Azulenoisindigo: A Building Block for π -Functional Materials with Reversible Redox Behavior and Proton Responsiveness

Bin Hou,^a Jing Li,^a Xiaodi Yang,^b Jianwei Zhang,^b Hanshen Xin,^a Congwu Ge,^a and Xike Gao*^a

^a Key Laboratory of Synthetic and Self-Assembly Chemistry for Organic Functional Molecules, Center for Excellence in Molecular Synthesis, Shanghai Institute of Organic Chemistry, University of Chinese Academy of Sciences, Chinese Academy of Sciences, 345 Lingling Road, Shanghai 200032, China.

Email: gaoxk@mail.sioc.ac.cn

^b Experiment Center for Science and Technology, Shanghai University of Traditional Chinese Medicine, 1200 Cai Lun Road, Shanghai 201203, China.

Abstract: Azulene, one of representative nonbenzenoid aromatic hydrocarbons, exhibits unique molecular structure and distinctive physical and chemical properties. Herein, an azulene-based isoindigo analogue, azulenoisindigo (**AzII**) is designed and synthesized, which has a twisted molecular backbone and R/S-isomers in single crystals. Interestingly, **AzII** shows the characteristics of both isoindigo and azulene, such as completely reversible redox behavior and reversible proton responsiveness. UV-vis-NIR, ¹H NMR and electron paramagnetic resonance (EPR) measurements were carried out to get insights into the possible mechanism of the proton-responsive property of **AzII**. The results demonstrated that only one azulenyl moiety of molecule of **AzII** was protonated and deprotonated, and the protonated **AzII** can be further oxidized to form azulenium cation radicals.

Azulene, a typical bicyclic nonbenzenoid aromatic system, can be regarded as the fusion of an electron-rich five-membered ring and an electron-deficient seven-membered ring (Fig. 1a). This nonalternant chemical structure distinguish azulene from the isomeric naphthalene, which endows azulene with a bright blue

color and a large dipole moment of 1.08 D.¹ In addition, the highest occupied molecular orbital (HOMO) and lowest unoccupied molecular orbital (LUMO) of azulene are different from those of naphthalene, showing a non-mirror-related electron density distribution.² This distinctive frontier orbital characteristics enable azulene with a small energy gap. Thanks to these unique structural and electronic configurations, azulene derivatives have been studied in functional organic materials³ including sensory materials,⁴ Near IR (NIR) materials,⁵ organic field-effect transistors (OFETs)⁶ and solar cells⁷. In recent years, more and more attention has been paid to the azulene derivatives for their applications in responsive materials.⁸ To further explore new stimuli-responsive π -functional materials, it is imperative to develop new synthetic strategies for constructing novel azulene-based materials with proton responsiveness.

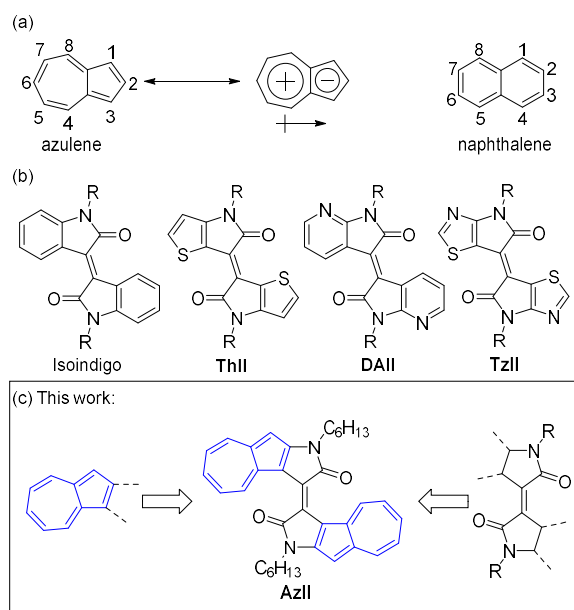


Fig. 1 Molecular structures of (a) azulene and naphthalene with atom number, (b) representative isoindigo analogues, and (c) **AzII**

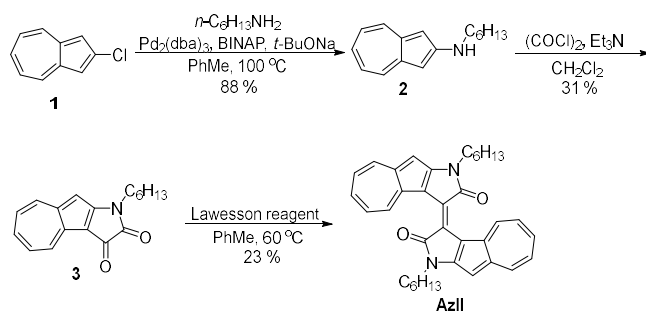
Isoindigo was identified as one of the most extensively studied moieties in optoelectronic materials.⁹ It has two five-membered lactam rings connected with an exocyclic double bond at the 3,3' positions and each lactam ring is fused with a benzene ring to form a conjugated structure. Since Reynolds and coworkers¹⁰ first investigated two isoindigo-based molecules in organic solar cells (OSCs) in 2010, isoindigo was soon widely applied as a building block to construct π -

functional materials.¹¹ Moreover, to explore the optoelectronic property and performance relationships of isoindigo analogues, some strategies have been developed to optimize the molecular structures^{9d}. Among them, one strategy is replacing the terminal phenyl rings with other aromatic rings. For example, the benzene rings were replaced by thiophene rings, pyridine rings and thiazole rings to form new isoindigo analogues, thienoisindigo (**ThII**),¹² diazaisoindigo (**DAII**)¹³ and thiazoloisoindigo (**TzII**),¹⁴ respectively (Fig. 1b). Through the molecular structure modification, the new isoindigo analogues perform even better optoelectronic properties than those of the intrinsic isoindigo.

In recent years, our group has devoted to the study of azulene-based π -functional materials.¹⁵ Herein we designed and synthesized a new isoindigo analogue, azulenoisoindigo (**AzII**), which combines the merits of azulene and isoindigo. As shown in Fig. 1c, the two lactam rings of **AzII** are fused with azulene at its 1,2-positions. The structural features and optoelectronic properties of **AzII** were explored by experimental measurements and theoretical calculations. It is worth noting that **AzII** possesses proton-responsive behavior, and would be a promising material used for sensors and other electronic devices.

The synthetic strategy of azulene-based isoindigo **AzII** is shown in Scheme 1. 2-chloroazulene (**1**) was prepared from commercially available tropolone according to the reported literature.¹⁶ Then compound **1** underwent Buchwald-Hartwig cross coupling reaction to afford *N*-hexylazulen-2-amine (**2**) in 88% yield. By using the high electrophilic aromatic substitution reactivity of 1-position in azulene, Friedel-Crafts acylation and amidation reaction of compound **2** with oxalyl chloride were performed under triethylamine affording the azulenoisatin **3** in 31% yield. The self-coupling reaction of azulenoisatin **3** using Lawesson reagent gave the targeted compound **AzII** in 23% yield. **AzII** showed good solubility in common organic solvents, such as CH₂Cl₂, CHCl₃, toluene and THF. The chemical structure of **AzII** was fully characterized with ¹H and ¹³C NMR spectroscopy, high-resolution mass spectrometry, FT-IR spectrometry, elemental analysis, as well as single crystal analysis. The decomposition

temperature of **AzII** was 302 °C defined as the 5% weight loss by a thermal gravimetric analysis (TGA), demonstrating the good thermal stability of **AzII**.



Scheme 1 Synthetic route of **AzII**

Single crystals of **AzII** grown by a slow diffusion method with dichloromethane and methanol solvents were characterized by single-crystal X-ray analysis. The single crystal analysis shows that **AzII** has an obvious twisted molecular backbone (Fig. 2). The dihedral angle of the two azulenyl moieties of **AzII** is 47.80°, which is larger than those of the previously described isoindigo analogues.¹⁷ It is noteworthy that there are *R/S* isomers in the crystal, which is probably due to the intense steric hindrance between the O atoms of lactam groups and the neighbouring H atoms at 4-position of azulenyl units. Attempts to separate the isomers by chiral HPLC failed, maybe due to the inversion of configuration of **AzII** at room temperature. The *R/S* isomers of **AzII** form a dimer through π - π stacking, and the interplanar distance is about 3.28 Å and the short intermolecular atom–atom contacts are among 3.36–3.37 Å between the two molecules in the dimer.

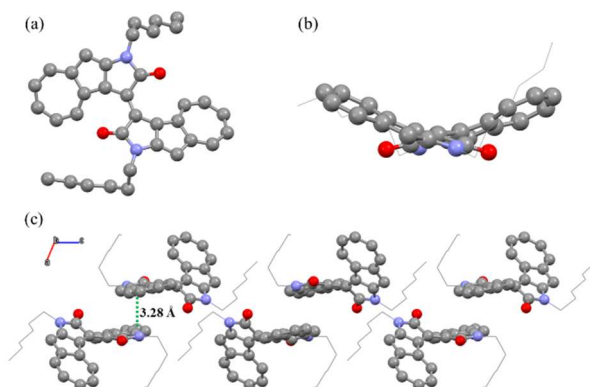


Fig. 2 Crystal structure of **AzII** (a) top view, (b) side view, and (c) molecular packing

To gain an insight into the molecular geometric structure and electronic properties of **AzII**, density functional theory (DFT) calculations were carried out at the B3LYP/6-31G(d,p) level using the Gaussian 16 Program. As depicted in Fig. 3, the optimized molecular geometry of **AzII** is twisted, which is consistent with that in the single crystals. The electron density distributions of both HOMO and LUMO are widely delocalized and spread over the whole π -conjugated backbone. The calculated HOMO and LUMO energy levels of **AzII** are -4.52 and -2.40 eV, respectively.

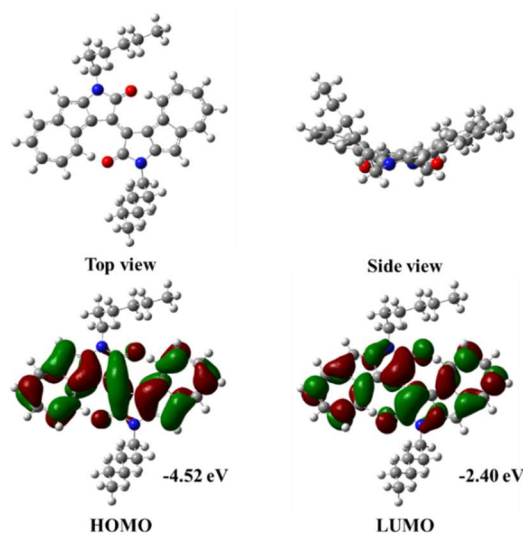


Fig. 3 Optimized molecular structure, frontier molecular orbitals and energy levels of **AzII** obtained by DFT calculations

The UV-vis-NIR absorption spectra and cyclic voltammetry (CV) of **AzII** were measured, and the related data are listed in Table 1. The UV-vis-NIR spectra of **AzII** in chloroform solution and in thin film are shown in Fig. 4a. **AzII** exhibits the broad absorption bands in the visible region with the end peak maxima at 664 nm ($\epsilon = 25500 \text{ M}^{-1} \text{ cm}^{-1}$). The spectra of **AzII** in the thin film is red shifted with an end peak at 705 nm, demonstrating the increased intramolecular conjugation and intermolecular π - π stacking in the thin film. The optical energy gap of **AzII** is calculated to be 1.60 eV from the onset of the end absorption in solution. The spectra of **AzII** are similar to those of other isoindigo analogues^{17a}, indicating that the spectral features of **AzII** was dominated by parent isoindigo structure.

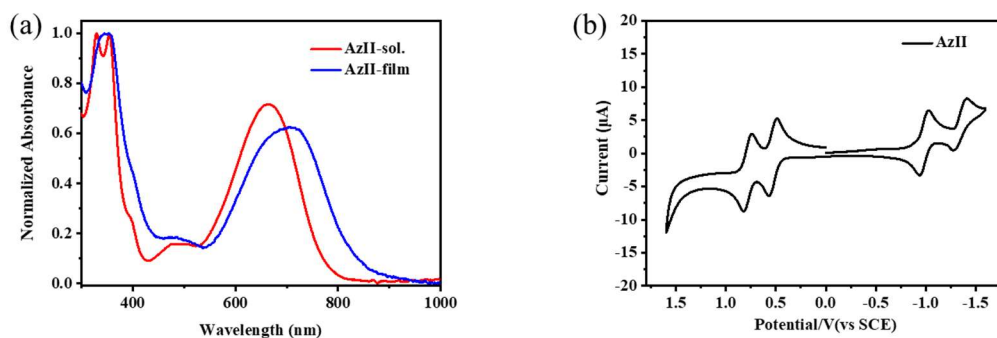


Fig. 4 (a) UV-vis-NIR absorption spectra of **AzII** in chloroform and in thin film, (b) cyclic voltammograms of **AzII** in dichloromethane ($0.1 \text{ mol L}^{-1} \text{ Bu}_4\text{NPF}_6$ as supporting electrolyte, SCE as reference electrode, scan rate of 100 mV s^{-1})

The electrochemical properties of **AzII** was investigated by CV in dichloromethane solution using $0.1 \text{ M Bu}_4\text{NPF}_6$ as the supporting electrolyte. As shown in Fig. 4b, **AzII** presents two reversible reduction waves with the first and second half-wave potentials ($\phi_{1/2}^{\text{red}}$ vs SCE) at -0.98 and -1.35 V , respectively. In the positive potential region, there are also two reversible oxidation processes with the first and second half-wave potentials ($\phi_{1/2}^{\text{ox}}$) vs SCE of 0.53 and 0.78 V , respectively. The HOMO and LUMO energy levels of **AzII** estimated by CV (energy level of ferrocene was assumed to be -4.80 eV versus vacuum¹⁸) are -4.89 and -3.38 eV , respectively. The resulting band gap (E_g^{CV}) is 1.51 eV , which is consistent with the optical bandgap (1.60 eV) with a deviation of 0.09 eV .

Table 1 Optical, electrochemical and DFT calculation data for **AzII**

Compound	$\lambda_{\text{max}}/\text{nm}$		$E_g^{\text{opt}}/a/$	$\phi_{1/2}^{\text{red1}}/b/$	$\phi_{1/2}^{\text{ox1}}/b/$	$E_{\text{HOMO}}^c/E_{\text{LUMO}}^c/$	$E_g^{\text{CV}}/d/$	$E_{\text{HOMO}}^e/E_{\text{LUMO}}^e/$	$E_g^{\text{cal}}/e/$
	Sol.	Film	eV	V	V	eV	eV	eV	eV
AzII	329, 354, 664	354, 705	1.60	-0.98	0.53	-4.89 -3.38	1.51	-4.52 -2.40	2.12

^a Estimated from the onset absorption of the solution; ^b First half-wave potential versus SCE; ^c Calculated from $E_{\text{HOMO/LUMO}} = -4.80 - \phi_{1/2}^{\text{ox1/red1}}$; ^d Calculated from CV; ^e Estimated from DFT calculations.

Conjugated polymers and small molecule containing azulene moieties are known to be sensitive to strong organic acids such as trifluoroacetic acid (TFA) owing to the protonation of 1- or 3-position of the azulene unit.⁸ To test the

proton-responsive properties of **AzII**, TFA was added to its dichloromethane solution (Fig. 5). The color of **AzII** solution changed obviously from sky blue to greyish green, which can be distinguished by naked eye. The color immediately recovered after neutralization with triethylamine (TEA). To clarify the color change, the UV-vis-NIR absorption of **AzII** upon protonation with various volume ratios of TFA was studied (Fig. 5). With the increase of volume ratios of TFA, the intensity of the absorption band at 664 nm decreased gradually. Meanwhile, a new band at 818 nm with a shoulder peak at 750 nm appeared, which was attributed to the protonation of **AzII**. When the TFA concentration was over 3% (*V/V*), the spectra did not change any more, suggesting the protonation state of **AzII** has reached saturation. An attempt to characterize the UV-vis-NIR absorption spectra of protonated **AzII** in thin film failed because of the formation of liquid drop when the thin film of **AzII** was protonated by using TFA vapor.

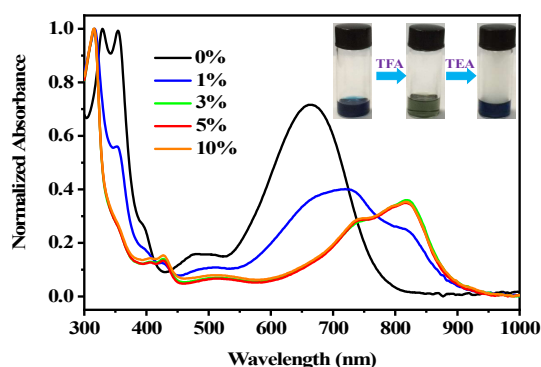


Fig. 5 Variations of UV-vis-NIR absorption spectra of **AzII** upon the protonation by TFA in chloroform

To further investigate the mechanism of the proton-responsive feature of **AzII**, ^1H NMR measurements of **AzII** in the neutral and protonated state were carried out. As shown in Fig. 6, ^1H NMR spectrum of **AzII** was broadened at aromatic regions after adding excessive TFA, whereas the split is obvious in the neutral state. Importantly, the proton signal at 3.86 ppm assigned to the CH_2 group linked with the N atom became chemical shift nonequivalence upon protonation, indicating that perhaps only one azulenyl moiety of **AzII** was protonated in the

presence of excessive TFA. When the acid-doped **AzII** was neutralized with TEA and washed with water, the ^1H NMR spectra of **AzII** recovered well to the initial state, demonstrating the reversible proton-responsive features of **AzII**. It is known that azulene derivatives are easily oxidized after protonation to form azulenium cation radicals. Thus, a study of electron paramagnetic resonance (EPR) was conducted with the neutral and TFA-protonated **AzII** in chloroform (Fig. S2, Table S1). Consequently, the **AzII** solution did not display any EPR signal in the neutral state, whereas a well-resolved symmetric signal with g -factor value of 2.0022 and a peak-to-peak line width (ΔH_{pp}) of 7.81 G appeared after the protonation of **AzII** in solution with TFA. The quantitative EPR experiment demonstrated that only about 2.1% of TFA-protonated **AzII** converted to azulenium cation radicals, thus the protonated **AzII** still showed good NMR signals and can be neutralized by TEA. These results are consistent with previous reports of azulene-based systems.⁸ As shown in Scheme S1, all results proposed that **AzII** possesses reversible proton responsiveness with only one azulenyl moiety of molecule protonated and the protonated **AzII** subsequently suffered from oxidation leading to cation radicals. This result demonstrates that **AzII** may be a potential building block for stimuli-responsive materials.

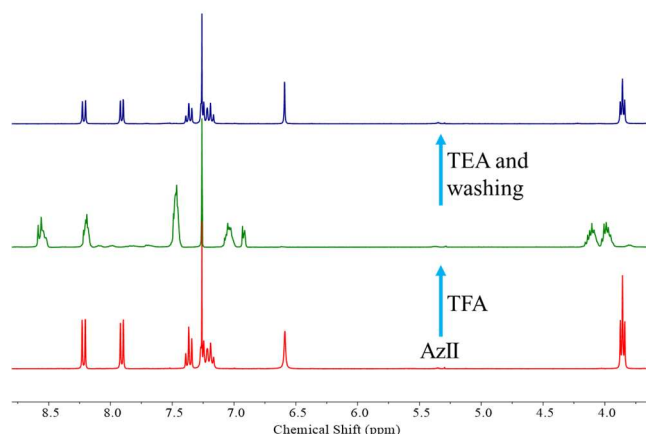


Fig. 6 ^1H NMR spectra of **AzII** in chloroform by acid doping and base dedoping

In conclusion, we have designed and synthesized an azulene-based isoindigo analogue **AzII**, which has a twisted backbone and axial chirality in single-crystal structure. DFT calculations, optical and electrochemical properties, as well as

proton responsiveness of **AzII** were investigated. **AzII** integrates the properties of isoindigo and azulene, shows reversible redox behavior and proton responsiveness. The UV-vis-NIR, ¹H NMR and EPR measurements demonstrated that only one azulenyl moiety of molecule of **AzII** was protonated and deprotonated, and the protonated **AzII** can be further oxidized to form azulonium cation radicals. Our work sheds light on the significance of incorporating azulenyl moiety into classical conjugated system, and **AzII** would be a promising building block for novel π -Functional materials. Further studies of **AzII**-based π -Functional materials are ongoing in our lab.

Acknowledgments

This research was financially supported by the National Natural Science Foundation of China (21790362 and 21522209), the “Strategic Priority Research Program of Chinese Academy of Sciences” (XDB12010100), the Science and Technology Commission of Shanghai Municipality (19XD1424700 and 18JC1410600) and SIOC.

References

- 1 (a) A. G. Anderson and B. M. Steckler, *J. Am. Chem. Soc.*, 1959, **81**, 4941; (b) G. W. Wheland and D. E. Mann, *J. Chem. Phys.*, 1949, **17**, 264.
- 2 J. Michl and E. W. Thulstrup, *Tetrahedron*, 1976, **32**, 205.
- 3 (a) J.-X. Dong and H.-L. Zhang, *Chin. Chem. Lett.*, 2016, **27**, 1097; (b) S. Ito and N. Morita, *Eur. J. Org. Chem.*, 2009, 4567; (c) L. Ou, Y. Zhou, B. Wu and L. Zhu, *Chin. Chem. Lett.*, 2019, **30**, 1903; (d) H. Xin and X. Gao, *ChemPlusChem*, 2017, **82**, 945.
- 4 (a) N. He, R. E. Gyurcsanyi and T. Lindfors, *Analyst*, 2016, **141**, 2990; (b) N. He, L. Hoefler, R.-M. Latonen and T. Lindfors, *Sens. Actuators B*, 2015, **207**, 918; (c) L. C. Murfin, C. M. Lopez-Alled, A. C. Sedgwick, J. Wenk, T. D. James and S. E. Lewis, *Front. Chem. Sci. Eng.*, 2020, **14**, 90.
- 5 (a) T. Tang, G. Ding, T. Lin, H. Chi, C. Liu, X. Lu, F. Wang and C. He, *Macromol. Rapid Commun.*, 2013, **34**, 431; (b) T. Tang, T. Lin, F. Wang and C. He, *Polym.*

- Chem.*, 2014, **5**, 2980; (c) F. Wang, T. T. Lin, C. He, H. Chi, T. Tang and Y.-H. Lai, *J. Mater. Chem.*, 2012, **22**, 10448.
- 6 (a) Y. Shibuya, K. Aonuma, T. Kimura, T. Kaneko, W. Fujiwara, Y. Yamaguchi, D. Kumaki, S. Tokito and H. Katagiri, *J. Phys. Chem. C*, 2020, **124**, 4738; (b) Y. Yamaguchi, Y. Maruya, H. Katagiri, K.-i. Nakayama and Y. Ohba, *Org. Lett.*, 2012, **14**, 2316; (c) Y. Yamaguchi, K. Ogawa, K.-i. Nakayama, Y. Ohba and H. Katagiri, *J. Am. Chem. Soc.*, 2013, **135**, 19095; (d) Y. Yamaguchi, M. Takubo, K. Ogawa, K.-i. Nakayama, T. Koganezawa and H. Katagiri, *J. Am. Chem. Soc.*, 2016, **138**, 11335.
- 7 (a) H. Nishimura, N. Ishida, A. Shimazaki, A. Wakamiya, A. Saeki, L. T. Scott and Y. Murata, *J. Am. Chem. Soc.*, 2015, **137**, 15656; (b) T. Umeyama, Y. Watanabe, T. Miyata and H. Imahori, *Chem. Lett.*, 2015, **44**, 47; (c) J. Yao, Z. Cai, Z. Liu, C. Yu, H. Luo, Y. Yang, S. Yang, G. Zhang and D. Zhang, *Macromolecules*, 2015, **48**, 2039.
- 8 (a) E. Amir, R. J. Amir, L. M. Campos and C. J. Hawker, *J. Am. Chem. Soc.*, 2011, **133**, 10046; (b) E. Amir, M. Murai, R. J. Amir, J. S. Cowart, Jr., M. L. Chabinyk and C. J. Hawker, *Chem. Sci.*, 2014, **5**, 4483; (c) M. Murai, E. Amir, R. J. Amir and C. J. Hawker, *Chem. Sci.*, 2012, **3**, 2721; (d) M. Murai, S. Iba, H. Ota and K. Takai, *Org. Lett.*, 2017, **19**, 5585; (e) M. Murai, S.-Y. Ku, N. D. Treat, M. J. Robb, M. L. Chabinyk and C. J. Hawker, *Chem. Sci.*, 2014, **5**, 3753; (f) K. Tsurui, M. Murai, S.-Y. Ku, C. J. Hawker and M. J. Robb, *Adv. Funct. Mater.*, 2014, **24**, 7338; (g) X. Wang, J. K.-P. Ng, P. Jia, T. Lin, C. M. Cho, J. Xu, X. Lu and C. He, *Macromolecules*, 2009, **42**, 5534.
- 9 (a) P. Deng and Q. Zhang, *Polym. Chem.*, 2014, **5**, 3298; (b) X. Guo, A. Facchetti and T. J. Marks, *Chem. Rev.*, 2014, **114**, 8943; (c) T. Lei, J.-Y. Wang and J. Pei, *Acc. Chem. Res.*, 2014, **47**, 1117; (d) J.-L. Li, J.-J. Cao, L.-L. Duan and H.-L. Zhang, *Asian J. Org. Chem.*, 2018, **7**, 2147; (e) N. M. Randell and T. L. Kelly, *Chem. Rec.*, 2019, **19**, 973; (f) R. Stalder, J. Mei, K. R. Graham, L. A. Estrada and J. R. Reynolds, *Chem. Mater.*, 2014, **26**, 664; (g) E. Wang, W. Mammo and M. R. Andersson, *Adv. Mater.*, 2014, **26**, 1801.

- 10 J. Mei, K. R. Graham, R. Stalder and J. R. Reynolds, *Org. Lett.*, 2010, **12**, 660.
- 11 (a) T. Lei, Y. Cao, Y. Fan, C.-J. Liu, S.-C. Yuan and J. Pei, *Journal of the American Chemical Society*, 2011, **133**, 6099; (b) T. Lei, J.-H. Dou, Z.-J. Ma, C.-H. Yao, C.-J. Liu, J.-Y. Wang and J. Pei, *J. Am. Chem. Soc.*, 2012, **134**, 20025; (c) R. Stalder, J. Mei and J. R. Reynolds, *Macromolecules*, 2010, **43**, 8348.
- 12 R. S. Ashraf, A. J. Kronemeijer, D. I. James, H. Sirringhaus and I. McCulloch, *Chem. Commun.*, 2012, **48**, 3939.
- 13 (a) G. de Miguel, L. Camacho and E. M. García-Frutos, *J. Mater. Chem. C*, 2016, **4**, 1208; (b) J. Huang, Z. Mao, Z. Chen, D. Gao, C. Wei, W. Zhang and G. Yu, *Chem. Mater.*, 2016, **28**, 2209; (c) Y. Lu, Y. Liu, Y.-Z. Dai, C.-Y. Yang, H.-I. Un, S.-W. Liu, K. Shi, J.-Y. Wang and J. Pei, *Chem. Asian J.*, 2017, **12**, 302.
- 14 (a) C. Li, H.-I. Un, J. Peng, M. Cai, X. Wang, J. Wang, Z. Lan, J. Pei and X. Wan, *Chem. Eur. J.*, 2018, **24**, 9807; (b) C. Li, H. Zhang, S. Mirie, J. Peng, M. Cai, X. Wang, Z. Lan and X. Wan, *Org. Chem. Front.*, 2018, **5**, 442.
- 15 (a) B. Hou, J. Li, H. Xin, X. Yang, H. Gao, P. Peng and X. Gao, *Acta Chim. Sinica*, 2020, **78**, 788; (b) H. Gao, C. Ge, B. Hou, H. Xin and X. Gao, *ACS Macro Lett.*, 2019, **8**, 1360; (c) H. Xin, C. Ge, X. Jiao, X. Yang, K. Rundel, C. R. McNeill and X. Gao, *Angew. Chem. Int. Ed.*, 2018, **57**, 1322; (d) H. Xin, C. Ge, X. Yang, H. Gao, X. Yang and X. Gao, *Chem. Sci.*, 2016, **7**, 6701; (e) H. Xin, J. Li, C. Ge, X. Yang, T. Xue and X. Gao, *Mater. Chem. Front.*, 2018, **2**, 975; (f) H. Xin, J. Li, R.-Q. Lu, X. Gao and T. M. Swager, *J. Am. Chem. Soc.*, 2020, **142**, 13598; (g) H. Xin, J. Li, X. Yang and X. Gao, *J. Org. Chem.*, 2020, **85**, 70.
- 16 (a) R. N. McDonald and J. M. Richmond, *J. Org. Chem.*, 1975, **40**, 1689; (b) N. Tetsuo, S. Shuichi and M. Shingo, *Bull. Chem. Soc. Jpn.*, 1962, **35**, 1990.
- 17 (a) T. Hasegawa, M. Ashizawa and H. Matsumoto, *RSC Adv.*, 2015, **5**, 61035; (b) Y. K. Voronina, D. B. Krivolapov, A. V. Bogdanov, V. F. Mironov and I. A. Litvinov, *J. Struct. Chem.*, 2012, **53**, 413.
- 18 A. R. Brown, C. P. Jarrett, D. M. de Leeuw and M. Matters, *Synth. Met.*, 1997, **88**, 37.